European Journal of Medicinal Chemistry 90 (2015) 232–240

Contents lists available at ScienceDirect

European Journal of Medicinal Chemistry

journal homepage: http://www.elsevier.com/locate/ejmech

Original article

Discovery of novel VEGFR-2 inhibitors. Part II: Biphenyl urea incorporated with salicylaldoxime

Hongping Gao, Ping Su, Yaling Shi, Xiuxiu Shen, Yanmin Zhang, Jinyun Dong, Jie Zhang*

School of Pharmacy, Health Science Center, Xi'an Jiaotong University, No. 76, Yanta West Road, Xi'an, Shaanxi Province, 710061, PR China

ARTICLE INFO

Article history:
Received 14 May 2014
Received in revised form
11 November 2014
Accepted 16 November 2014
Available online 18 November 2014

Keywords:
VEGFR-2
Biphenyl urea
Intramolecular hydrogen bond
Salicylaldoxime

ABSTRACT

A series of novel VEGFR-2 inhibitors containing oxime as hinge binding fragment were described. A strategy of pseudo six-membered ring formed through intramolecular hydrogen bond was employed to mimic the planar quinazoline. The oxime group was firstly introduced to interact with hinge region of VEGFR-2. Most of compounds tested showed moderate to high VEGFR-2 inhibitory activity. In particular, **12l**, **12p** and **12y** exhibited significant enzymatic inhibitory activity as well as potent antiproliferative activity against cancer cells. Molecular docking suggested that the salicylaldoxime formed two hydrogen bonds with hinge region. These biphenylureas could serve as promising lead compounds for developing novel anticancer agents.

© 2014 Elsevier Masson SAS. All rights reserved.

1. Introduction

Tumor angiogenesis plays a central role in cancer cell survival, tumor growth, and the development of distant metastasis [1]. Numerous regulators of angiogenesis have been identified and characterized. Among them, vascular endothelial growth factor (VEGF) and receptor (VEGFR-2) are identified as positive regulators of pathological angiogenesis associated with tumors [2]. VEGFR-2 inhibition has been considered as effective strategy for the prevention of angiogenesis [3]. Antiangiogenic therapy based on VEGFR-2 inhibition is powerful clinical treatment of cancers and VEGFR-2 is becoming attractive target for anticancer drug discovery [4]. At present, many VEGFR-2 targeted agents have been approved for cancer therapy [5]. There are various structure elements of VEGFR-2 inhibitors (Fig. 1) such as urea (**Sorafenib**) [6], **ABT-869** [7]; 3-substituted indolinones (**Sunitinib**) [8]; 4-anilinoquinazolines (**ZD4190**) [9]. These outcomes encouraged us to develop novel VEGFR-2 inhibitors as promising anticancer agents [10].

To our knowledge, biphenyl urea and its derivatives are important fine chemicals. They have found extensive useful applications as tranquilizers and antibiotic drugs. Recently, we have described the synthesis and biological evaluation of biphenyl urea-based VEGFR-2 inhibitors (Fig. 2) [11]. Molecular docking indicated that the urea moiety formed four hydrogen bonds with DFG residue of VEGFR-2. The results confirmed as known that urea moiety played an essential role in enzymatic inhibitory activity. Moreover, these biphenylureas have strong potential to be further optimized.

In continuing our search for novel biphenyl ureas with potent VEGFR-2 inhibitory and anticancer activity, we extended the structural diversity of biphenyl ureas. In order to enhance the affinity for VEGFR-2, the methoxy group was converted to hydroxyl group while the acetyl group was optimized to oxime (Fig. 2). These salicylaldoximes form a pseudo six-membered ring *via* a hydrogen bond. They could mimic quinazoline of known ATP-competitive inhibitors [12]. The intramolecular hydrogen bond stabilizes planar conformation and makes the molecule considerable rigid. The conformational similarity of salicylaldoxime to quinazoline led to the hypothesis that both of them could act with hinge region of VEGFR-2.

Based on our previous promising results, we described the design, synthesis and biological evaluation of a series of biphenyl ureas as novel VEGFR-2 inhibitors. They displayed potent anticancer effect and could be considered as promising lead compounds for further optimization. A molecular dock model and preliminary SAR based on enzymatic inhibitory activity will also be discussed.

* Corresponding author.
E-mail address: zhj8623@mail.xjtu.edu.cn (J. Zhang).

http://dx.doi.org/10.1016/j.ejmech.2014.11.032
0223-5234/© 2014 Elsevier Masson SAS. All rights reserved.

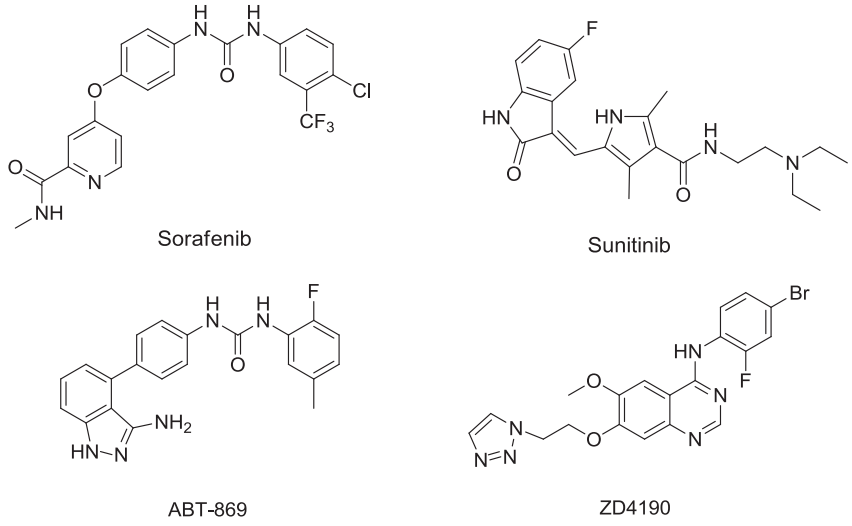

Fig. 1. VEGFR-2 inhibitors currently approved or in clinical trials.

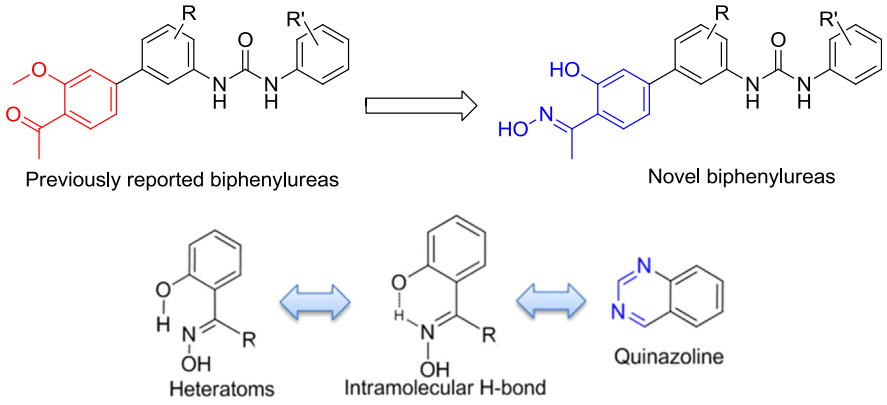

Fig. 2. Structures of title compounds with intramolecular hydrogen bonds and quinazoline.

2. Results and discussion

2.1. Chemistry

A convenient method for the synthesis of biphenyl ureas has been described before [13]. Based on our previous research, the general synthesis of title compounds was depicted in Scheme 1. Commercial available vanillin was converted into 2-bromovanillin by reaction with bromine [14], then aldehyde group was converted to cyano group *via* a one-pot oxime formation, dehydration, and subsequent *O*-methylation to afford (**2**). Compound (**3**) was obtained by methylation and hydrolysis of (**2**) with sodium formate and hydroxylamine sulfate in formic acid [15]. Then amide group was converted to amine through Hoffmann's degradation. Compound (**6**) was obtained by acylation of 3-bromophenol with acetic anhydride and Fries rearrangement [16]. Hydroxyl group of (**6**) was protected by benzyl to afford (**7**). Another intermediate (**8**) was prepared by coupling of bis(pinacolato)diboron with bromide (**7**) without further purification [17]. Critical intermediate (**9**) was prepared from (**8**) and (**4**) by classical Suzuki coupling reaction [18]. Subsequently, intermediate (**9**) was treated with triphosgene (BTC) to produce various isocyanate, followed by reacting with substituted anilines yielding (**10**) [19]. After deprotection of benzyl group, the title compounds (**12a**–**12y**) were obtained by subsequent condensation of (**11**) with hydroxylamine hydrochloride.

2.2. Biological evaluation

The entire library of title compounds was evaluated against VEGFR-2 with Sorafenib as positive control (Table 1). As shown in Table 1, the majority of them displayed moderate to high VEGFR-2 inhibitory activity. Among them, **12l**, **12p**, **12y** potently inhibited VEGFR-2 with nanomolar potency (IC_{50} = 8.7 nM, 5.3 nM, 4.2 nM).

Biphenyl ureas incorporated with 2-fluorine substituent on terminal aniline displayed more potent activity than the others. They showed potent VEGFR-2 inhibitory activity with IC_{50} values ranging from 5.3 nM to 549.0 nM. **12l** and **12p** exhibited high potency with IC_{50} values of 8.7 nM and 5.3 nM, respectively. Compounds with hydrogen and methyl substituent on terminal benzene displayed moderate or poor activity. **12f** was the most potent in these two series with IC_{50} value of 13.0 nM. Biphenyl ureas with 2-chlorine substituent also exhibited potent activity with IC_{50} values ranging from 55.9 nM to 949.0 nM.

In order to identify the importance of the *o*-hydroxyl group, three biphenylureas (**12w′**–**12y′**) without hydroxy group were synthesized and evaluated (Table 2). As shown in Table 2, the incorporation of the hydroxy into the ortho position of oxime resulted in an increase of potency. The salicylaldoximes (**12w**–**12y**) exhibited potent activities which were 10- to 60-fold higher than their precursor (**12w′**–**12y′**), especially for **12y** which is the most potent VEGFR-2 inhibitor with IC_{50} value of 4.2 nM. These results

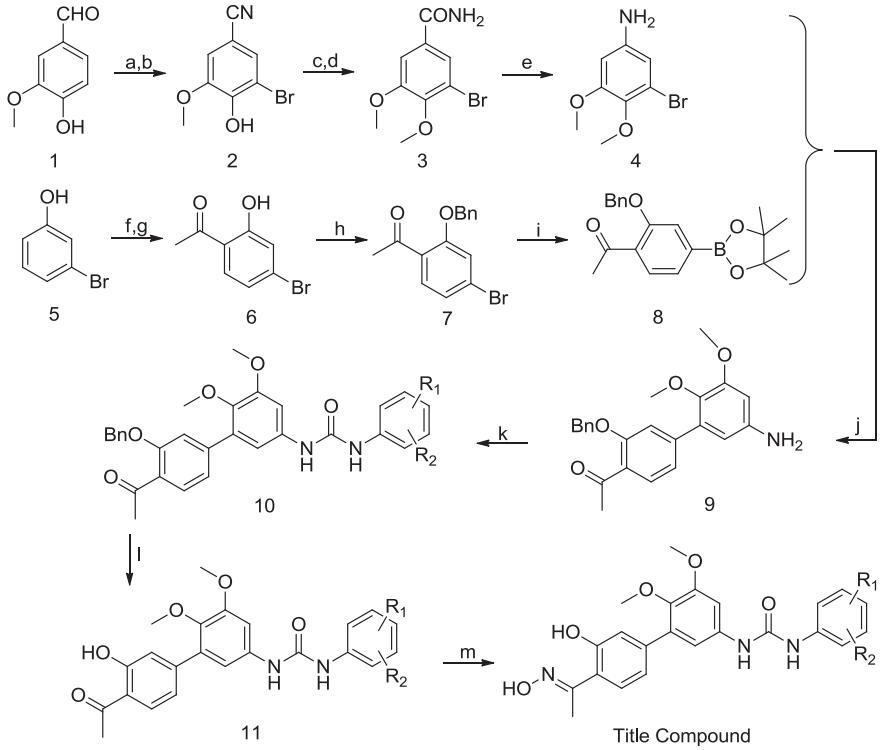

Scheme 1. Synthetic route of biphenyl ureas. **Reagents and conditions**: **a**: Br_2, AcOH, AcONa, Fe, rt; **b**: HCOOH, HCOONa, $(NH_3OH)_2SO_4$, 90 °C; **c**: $(CH_3)_2SO_4$, K_2CO_3, Me_2CO, 50 °C; **d**: H_2O_2, NaOH, EtOH, 60 °C; **e**: Br_2, NaOH; **f**: Py, Ac_2O, rt; **g**: $AlCl_3$,160 °C; **h**: BnCl, K_2CO_3, DMF, 100 °C; **i**: $B_2O_4(CH)_4(CH_3)_8$, dioxane, $Pd(pddf)Cl_2$, KOAc, 100 °C; **j**: Na_2CO_3, H_2O, dioxane,100 °C; **k**: BTC, substituted anilines, Et_3N, DCM, rt; **l**: Pd/C, MeOH, rt; **m**: EtOH, NH_4OH, H_2O.

indicated that the intramolecular hydrogen bond might be essential for the VEGFR-2 inhibitory activity.

Eight selected biphenyl ureas were evaluated for their antiproliferative activity against nine cancer cell lines with Sunitinib as a standard. Their activity was measured by 3-(4,5-dimethylthiazol-2-yl)-2,5-diphenyltetrazolium bromide (MTT) method. The anticancer potency (IC_{50}) of them was shown in Table 3. The IC_{50} values were the average of at least three independent experiments. Majority of title compounds could inhibit the growth of cancer cell lines in a dose-dependent manner. It was observed from Table 3 that **12p** displayed the most potent antiproliferative activity against five cancer cell lines comparable to that of Sunitinib. In particular, it showed higher potency against MDA-MB-435S with IC_{50} value of 0.35 μM.

2.3. Molecular docking study

A deeper structural interpretation of above biological results is required for further optimization. In order to obtain more understanding of the interaction with receptor, a molecular modeling study was performed using Sybyl-X 2.0. The most potent inhibitor (**12p**) was docked into ATP binding site of VEGFR-2 (PDB ID: 3C7Q). We chose **12p** because, according to the biological results presented in the previous section, it is one of the most potent compounds. Molecular insights based on docking indicated favorable binding interactions of **12p** with the active site of VEGFR-2 (Fig. 3). We found that hydroxy group of oxime formed two hydrogen bonds to Cys917 with distance of 2.05 Å and 1.97 Å, respectively. Carbonyl group of urea was identified to be involved in hydrogen bond with the backbone NH of Asp 1044 with distance of 2.21 Å. The salicylaldoxime moiety bound to the hinge region (Cys917) of VEGFR-2, while the urea was sandwiched between the activation loop of Asp1044 and Glu883.

3. Conclusion

In conclusion, twenty-eight biphenyl ureas were designed and synthesized using a convergent synthetic route. These compounds allowed us to introduce efficiently structural diversity at biphenyl scaffold, especially at the moiety binding with hinge region. The majority of them exhibited moderate to high inhibitory activity against VEGFR-2. Three of them (**12l**, **12p** and **12y**) displayed significant enzymatic inhibitory activities, with IC_{50} values of 8.7 nM, 5.3 nM and 4.2 nM. Moreover, **12p** showed great antiproliferative potency against A549, MCF-7, MDA-MB-435S, MDA-MB-231 and HT29 cell lines. Docking study indicated three hydrogen bonds between urea unit and salicylaldoxime with VEGFR-2. It could be verified that the pseudo six-membered ring formed by intramolecular hydrogen bond played important role in biological activity. These results suggested that not only urea moiety but also salicylaldoxime were benefit for their anticancer potency. These biphenyl ureas may possibly be used as lead compounds for developing novel VEGFR-2 inhibitors. Further structural optimization of these promising anticancer agents will be reported in due course.

4. Experimental section

4.1. Chemistry

4.1.1. General procedure

Solvents and reagents are purified according to the standard procedure. Reactions are monitored by thin layer chromatography on 0.25-mm silica gel plates (60GF-254) and visualized with UV light. The reactions except those in aqueous media are carried out by standard techniques for the exclusion of moisture. Melting points are determined on electrothermal melting point apparatus

Table 1
Structure and VEGFR-2 inhibitory activity of biphenyl ureas.

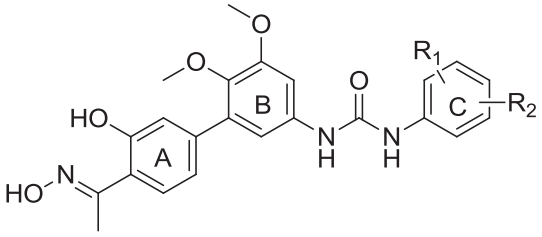

Compound	R_1	R_2	IC_{50}, nM	Compound	R_1	R_2	IC_{50}, nM
12a	H	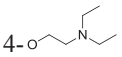	ND[a]	12n	2-F	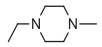	247.0
12b	H	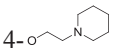	225.0	12o	2-F	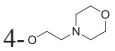	365.9
12c	H	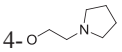	197.6	12p	2-F	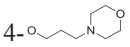	5.3
12d	H	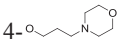	240.0	12q	2-Cl	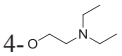	141.2
12e	2-CH_3	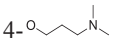	ND	12r	2-Cl	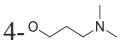	55.9
12f	2-CH_3	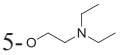	13.0	12s	2-Cl	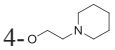	435.1
12g	2-CH_3	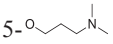	ND	12t	2-Cl	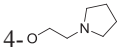	949.0
12h	2-CH_3	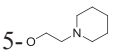	63.0	12u	2-Cl	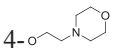	300.8
12i	2-CH_3	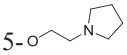	270.0	12v	2-Cl	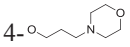	615.1
12j	2-CH_3	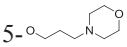	ND	12w	H		18.4
12k	2-F	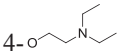	43.2	12x	H		78.7
12l	2-F	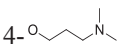	8.7	12y	H	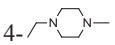	4.2
12m	2-F	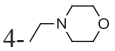	549.0	Sorafenib			2.2

[a] ND = not determined.

and are uncorrected. ^{1}H NMR spectra are measured at 400 MHz on a Bruker Advance AC 400 instrument. Mass spectra are obtained on a Shimadzu HPLC-MS-QP2010 instrument.

*4.1.2. 3-bromo-4-hydroxy-5-methoxybenzonitrile (**2**)*

To a mixture of (**1**) (30.0 g, 0.20 mol), NaOAc (33.0 g, 0.40 mol) and iron power (1.05 g, 0.02 mol) was added glacial acetic acid (180 mL). The mixture was stirred at room temperature for 30 min. Br_2 (10.5 mL, 0.021 mol) in glacial acetic acid (40 mL) was added dropwise at 23–25 °C. The mixture was stirred at the same temperature overnight. Ice-water (300 mL) was added and stirred for another one hour. The solid obtained was dried and recrystallized from EtOH to give gray solid. A mixture of the obtained solid (23.0 g, 100 mmol), sodium formate (12.6 g, 200 mmol), and formic acid (150 mL) was heated to 90 °C. Then hydroxylamine sulfate (9.80 g, 60 mmol) was added in five equal portions at 30 min intervals, and the mixture was heated at 90 °C for 5 h. The reaction was cooled to room temperature and poured to a solution of sodium chloride (120 g) in water (600 mL). The resultant solid was collected by filtration, washed with water, and dried to give (**2**) (18.92 g, 84%) as off-white solid. Mp: 159–160 °C, MS (EI) $[M]^+$: $m/z = 230$, ^{1}H NMR (400 MHz, $CDCl_3$) δ ppm: 7.38 (s, 1H), 6.62 (s, 1H), 4.00 (s, 3H).

*4.1.3. 3-bromo-4,5-dimethoxybenzamide (**3**)*

A mixture of (**2**) (16.0 g, 70 mmol), potassium carbonate (32.1 g, 0.23 mol) and acetone (150 mL) was stirred at 50 °C for 30 min. Dimethyl sulfate (13.9 mL, 0.15 mol) was added dropwise at 50 °C. After completion of reaction, the solid was filtered off and the solvent was evaporated. The solid obtained was dried to give off-white solid. To a solution of the obtained solid (13.3 g, 55 mmol) in ethanol (200 mL) was added NaOH (2.42 g, 60.5 mmol) and 30% H_2O_2 (22 mL, 0.93 mol). The mixture was stirred at 60 °C for 1 h and

Table 2
Structure and VEGFR-2 inhibitory activity of biphenyl ureas without intramolecular hydrogen bonds.

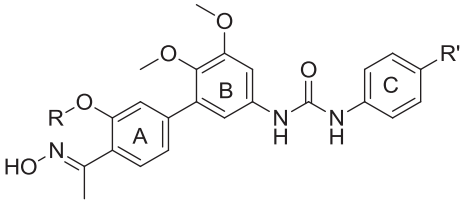

Compound	R	R′	IC_{50}, nM	Compound	R	R′	IC_{50}, nM
12w	H		18.4	12w′	Me		235.3
12x	H		78.7	12x′	Me		1580.0
12y	H		4.2	12y′	Me		256.3

acidified with concentrated HCl. Ethanol was evaporated and residues was poured into water and filtered. The white solid obtain was dried to give (**3**) (12.40 g, 86.8%).

*4.1.4. 3-bromo-4,5-dimethoxyphenylamine (**4**)*

Br_2 (1.35 mL) was added dropwise into a solution of NaOH (4.0 g, 100 mmol) in distilled water (81 mL) at −5 °C and was stirred for another 10 min. Compound (**3**) (5.40 g, 21 mmol) was added into the above solution in batches and stirring continued for 20 min. The mixture was warmed to r.t. and kept for 30 min. Then the suspension was heated at 40 °C for 1 h. The mixture was cool to r.t. and was poured into water and extracted with AcOEt (50 mL × 3). The organic layer was collected and washed with water, brine, and dried over Na_2SO_4. Filtration and concentration *in vacuo* afford crude product. Further purification by silica gel flash chromatography (PE/AcOEt = 2:1) gave (**4**) (2.62 g, 54%) as yellow solid.

*4.1.5. 1-(4-Bromo-2-hydroxyphenyl)ethanone (**6**)*

3-Bromophenol (**5**) (10.0 g, 58 mmol) was dissolved in pyridine (30 mL) under ice-bath and was stirred for 30 min. Acetic anhydride (8.3 mL, 88 mmol) was added dropwise into above mixture at the same temperature. The ice-bath was removed after dropping and the mixture was stirred for 2 h. Concentrated HCl and ice-water (300 mL) was added to neutralize PH to 7. The mixture was extracted with AcOEt (100 mL × 3). The organic layer was collected and washed with brine and dried over Na_2SO_4. Filtration and concentration *in vacuo* afforded yellow oil. In a 250 mL round bottom flask, the obtained yellow oil (6.45 g, 30 mmol) and anhydrous $AlCl_3$ (12.02 g, 90 mmol) was mixed at 160 °C for three hours. Reaction mixture was poured into ice water and concentrated hydrochloric acid solution was added to break complex formed during reaction. The mixture was taken in AcOEt (50 mL × 3). The organic layer was combined and washed with water and brine, and dried over Na_2SO_4. After filtration and concentration *in vacuo*, the residues was purified by silica gel flash chromatography (PE/AcOEt = 30:1) give (**6**) (4.74 g, 73.5%) as white solid.

*4.1.6. 1-[2-(benzyloxy)-4-bromophenyl]ethanone (**7**)*

To a mixture of (**6**) (4.3 g, 20 mmol), potassium carbonate (8.28 g, 60 mmol) and DMF (60 mL) was added Benzyl chloride (2.78 mL, 22 mmol), stirred for 1 h at 100 °C under the atmosphere of nitrogen. Ice-water (240 mL) was added to the mixture and stirred for another 30 min. The resultant solid was collected by filtration, washed with water, and dried to give (**7**) (5.18 g, 85%) as an off-white solid.

*4.1.7. 1-[5′-amino-3-(benzyloxy)-2′,3′-dimethoxybiphenyl-4-yl] ethanone (**9**)*

A flask charged with Pd(pddf)Cl_2 (0.48 g, 0.65 mmol), KOAc (2.57 g, 26 mmol), and the bis(pinacolato)diboron (1.82 g, 7.2 mmol) and compound (**7**) (2 g, 6.5 mmol) was flushed with nitrogen. 1,4-dioxane (30 mL) was then added. After being stirred at 100 °C for 5 h under nitrogen atmosphere, the mixture was cooled to afford the black oil mixture without further purified. Compound (**4**) (1.21 g, 5.2 mmol), sodium carbonate (1.39 g, 13.1 mmol), H_2O (7 mL) and 1,4-dioxane (5 mL) were then added to the mixture. It was then refluxed overnight under nitrogen. The product was extracted with AcOEt (50 mL × 3), washed with water, and dried over Na_2SO_4. After filtration and concentration *in vacuo*, the residues was purified by silica gel flash chromatography (PE/AcOEt = 3:1) gave (**9**) (1.55 g, 63%) as slight yellow solid.

*4.1.8. N-[4′-acetyl-3′-(benzyloxy)-5,6-dimethoxybiphenyl-3-yl]-N′-{4-[2-(diethylamino)ethoxy]phenyl}urea (**10**)*

Triphosgene (0.47 g, 1.6 mmol) was dissolved in anhydrous CH_2Cl_2 (25 mL) and the mixture was stirred on the ice-bath for 15 min. A solution of the (**9**) (1.50 g, 4 mmol) in anhydrous CH_2Cl_2 (10 mL) was added dropwise to the above mixture and stirring continued for 15 min. Et_3N (0.48 mL, 3.44 mmol) diluted with CH_2Cl_2 (5 mL) was then added into the mixture. Stirring was continued for 15 min and a solution of Et_3N (0.48 mL, 3.44 mmol), 4-(2-diethylamino-ethoxy)-phenylamine (0.83 g, 4 mmol) in anhydrous CH_2Cl_2 (25 mL) was added. After completion of the action, the reaction was quenched with dilute $NaHCO_3$. The organic layer was washed with water and brine, and dried over Na_2SO_4. After filtration and concentration *in vacuo*, the residues was purified by silica gel flash chromatography (CH_2Cl_2/MeOH = 30:1) gave as yellow solid (**10**) (0.87 g, 35%).

*4.1.9. N-(4′-acetyl-3′-hydroxy-5,6-dimethoxybiphenyl-3-yl)-N′-{4-[2-(diethylamino) ethoxy]phenyl}urea (**11**)*

To a solution of (10) (0.61 g, 1 mmol) in methanol (20 ml) was added Pd/C (0.03 g, 0.3 mmol), stirred for 24 h in room temperature under the atmosphere of hydrogen. The mixture was filtered to remove Pd/C, after filtration and concentration *in vacuo* to give (**11**) (0.44 g, 85%) as slight yellow solid.

*4.1.10. N-{4-[2-(diethylamino)ethoxy]phenyl}-N′-{3′-hydroxy-4′-[(1E)-N-hydroxyethanimidoyl]-5,6-dimethoxybiphenyl-3-yl}urea (**12a**)*

Compound (**11**) (0.40 g, 0.7 mmol) was dissolved in ethanol 20 mL and the solution was heated to 50 °C. After being stirred for 15 min, hydroxylamine hydrochloride was added to the above mixture and stirring continued for 5 h. The mixture was poured into cool water and neutralized with $NaHCO_3$. The product was extracted with CH_2Cl_2 (20 mL × 3), washed with water, and dried over Na_2SO_4. Filtration and concentration *in vacuo* afford **12a** (0.36 g, 87%) as slight yellow solid. mp: 117–119 °C. EI-MS (*m*/*z*): 536.3 (M^+). ^1H NMR (400 MHz, $(CD_3)_2SO$) δ 11.64 (s, 1H), 11.61 (s, 1H), 8.62 (s, 1H), 8.48 (s, 1H), 7.54 (d, J = 4 Hz, 1H), 7.35 (s, 1H), 7.33 (s, 1H), 7.25 (s, 1H), 7.01 (d, J = 4 Hz, 1H), 6.98 (s, 1H), 6.95 (s, 1H), 6.87 (s, 1H), 6.85 (s, 1H), 3.97 (t, J = 6 Hz, 2H), 3.83 (s, 3H), 3.50 (s, 3H), 2.76 (t, J = 6 Hz, 2H), 2.56 (m, J = 8 Hz, 4H), 2.30 (s, 3H), 0.98 (t, J = 6 Hz, 6H).

Title compounds **12b**–**12y′** were prepared by using the general procedure described above.

Table 3
Antiproliferative activities of title compounds on cancer cells.

Compound	Cancer cell lines, IC_{50} (μM)								
	A549	MCF-7	ECV304	MDA-MB-435S	H1299	MDA-MB-231	A375	HT29	SMMC-7721
Sunitinib	3.99	9.81	1.90	4.78	1.76	4.55	2.12	2.63	3.21
12b	4.29	15.89	4.64	1.65	7.57	4.98	5.85	8.16	9.28
12c	4.67	ND[a]	4.98	16.06	3.84	3.88	ND	6.57	ND
12f	5.30	12.91	3.46	12.09	3.16	10.01	ND	6.54	27.65
12k	2.55	13.01	ND	6.68	3.63	5.13	4.99	6.83	31.00
12l	3.96	9.68	ND	ND	2.63	5.32	3.96	3.40	28.40
12p	2.03	9.52	6.25	0.35	19.09	3.73	2.44	2.04	6.55
12r	3.91	10.71	3.64	12.86	4.04	5.48	2.30	4.33	15.18
12y	ND	4.75	ND	67.58	6.82	4.13	2.37	14.97	2.87

[a] ND = Not determined.

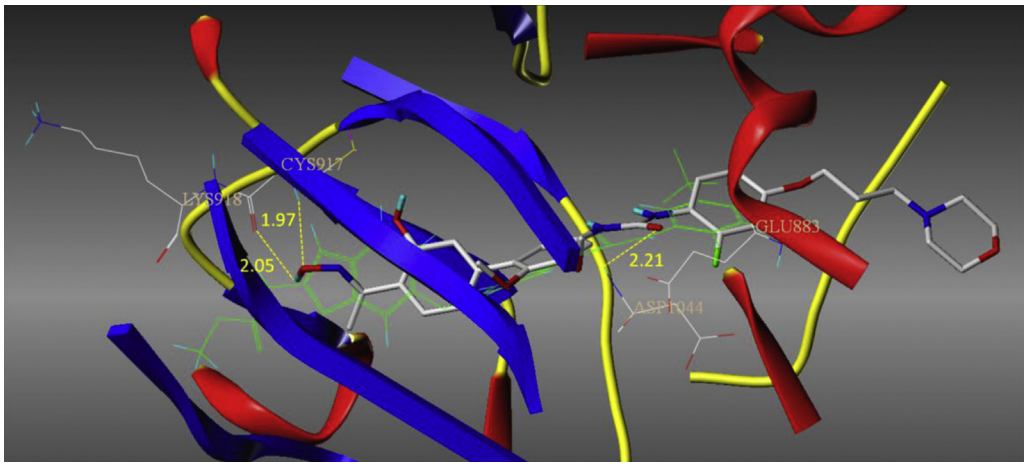

Fig. 3. The structure of VEGFR-2 ATP site in complex with compound (**12p**).

*4.1.10.1. N-{3′-hydroxy-4′-[(1E)-N-hydroxyethanimidoyl]-5,6-dimethoxybiphenyl-3-yl}-N′-[4-(2-piperidin-1-ylethoxy)phenyl]urea (**12b**).* mp.: 131–133 °C. EI-MS (*m/z*): 548.3 (M^+). ^{1}H NMR (400 MHz, $(CD_3)_2SO$) δ 11.64 (s, 1H), 11.62 (s, 1H), 8.79 (s, 1H), 8.65 (s, 1H), 7.54 (d, *J* = 4 Hz, 1H), 7.36 (s, 1H), 7.34 (s, 1H), 7.27 (s, 1H), 7.01 (d, *J* = 4 Hz, 1H), 6.98 (s, 1H), 6.95 (s, 1H), 6.89 (s, 1H), 6.87 (s, 1H), 4.06 (s, 2H), 3.82 (s, 3H), 3.50 (s, 3H), 2.74 (t, *J* = 22 Hz, 2H), 2.51 (s, 4H), 2.29 (s, 3H), 1.54 (s, 4H), 1.40 (s, 2H).

*4.1.10.2. N-{3′-hydroxy-4′-[(1E)-N-hydroxyethanimidoyl]-5,6-dimethoxybiphenyl-3-yl}-N′-[4-(2-pyrrolidin-1-ylethoxy)phenyl]urea (**12c**).* mp.: 121–122 °C. EI-MS (*m/z*): 534.2 (M^+). ^{1}H NMR (400 MHz, $(CD_3)_2SO$) δ 11.65 (s, 1H), 8.69 (s, 1H), 8.55 (s, 1H), 7.54 (d, *J* = 4 Hz, 1H), 7.47 (d, *J* = 4 Hz, 1H), 7.36 (s, 1H), 7.34 (s, 1H), 7.25 (d, *J* = 4 Hz, 1H), 7.01 (d, *J* = 4 Hz, 1H), 6.97 (d, *J* = 4 Hz, 1H), 6.87 (s, 1H), 6.85 (s, 1H), 4.01 (t, *J* = 6 Hz,2H), 3.48 (d, *J* = 6 Hz, 3H), 2.76 (t, *J* = 6 Hz, 2H), 2.51 (s, 4H), 2.29 (s, 3H), 1.68 (s, 4H).

*4.1.10.3. N-{3′-hydroxy-4′-[(1E)-N-hydroxyethanimidoyl]-5,6-dimethoxybiphenyl-3-yl}-N′-[4-(3-morpholin-4-ylpropoxy)phenyl] urea (**12d**).* mp.: 160–162 °C. EI-MS (*m/z*): 564.3 (M^+). ^{1}H NMR (400 MHz, $(CD_3)_2SO$) δ 11.64 (s, 1H), 11.62 (s, 1H), 9.34 (s, 1H), 9.18 (s, 1H), 7.54 (d, *J* = 4 Hz, 1H),7.38 (s, 1H), 7.36 (s, 1H), 7.31 (s, 1H), 7.00 (d, *J* = 4 Hz, 1H), 6.97 (s, 1H), 6.92 (s, 1H), 6.89 (s, 1H), 6.86 (s, 1H), 4.01 (t, *J* = 6 Hz, 2H), 3.86 (s, 4H), 3.82 (s, 3H), 3.49 (s, 3H), 3.16 (s, 6H), 2.29 (s, 3H), 2.14 (m, *J* = 12 Hz, 2H).

*4.1.10.4. N-{4-[3-(dimethylamino)propoxy]-2-methylphenyl}-N′-{3′-hydroxy-4′-[(1E)-N-hydroxyethanimidoyl]-5,6-dimethoxybiphenyl-3-yl}urea (**12e**).* mp.: 148–150 °C. EI-MS (*m/z*): 536.3 (M^+). ^{1}H NMR (400 MHz, $(CD_3)_2SO$) δ 11.69 (s, 1H), 9.78 (s, 1H), 8.50 (s, 1H), 7.53 (d, *J* = 4 Hz, 1H), 7.49 (d, *J* = 4 Hz, 1H), 7.34 (s, 1H), 7.00 (d, *J* = 4 Hz, 1H), 6.97 (s, 2H), 6.76 (s, 1H), 6.70 (m, *J* = 6 Hz, 1H), 3.94 (t, *J* = 6 Hz, 2H), 3.82 (s, 3H), 3.49 (s, 3H), 2.34 (t, *J* = 8 Hz, 2H), 2.29 (s, 3H), 2.22 (s, 3H), 2.14 (s, 6H), 1.83(t, *J* = m, 10 Hz,2H).

*4.1.10.5. N-{5-[2-(diethylamino)ethoxy]-2-methylphenyl}-N′-{3′-hydroxy-4′-[(1E)-N-hydroxyethanimidoyl]-5,6-dimethoxybiphenyl-3-yl}urea (**12f**).* mp.: 160–161 °C. EI-MS (*m/z*): 550.2 (M^+). ^{1}H NMR (400 MHz, $(CD_3)_2SO$) δ 9.46 (s, 1H), 8.09 (s, 1H), 7.57 (s, 1H), 7.53 (d, *J* = 4 Hz, 1H), 7.25 (s, 1H), 7.03 (d, *J* = 6 Hz, 2H), 7.00 (s, 1H), 6.98 (s, 1H), 6.50 (m, *J* = 6 Hz, 1H), 3.94 (t, *J* = 6 Hz, 2H), 3.84 (s, 3H), 3.50 (s, 3H), 2.75 (t, *J* = 6 Hz, 2H), 2.54 (m, *J* = 12 Hz, 4H), 2.29 (s, 3H), 2.17 (s, 3H), 0.97 (t, *J* = 8 Hz, 6H). ^{13}C NMR (101 MHz, $(CD_3)_2SO$) δ 157.62, 157.45, 157.24, 153.29, 153.12, 141.16, 140.31, 138.74, 136.58, 134.54, 131.01, 128.13, 120.06, 119.11, 118.77, 117.25, 111.35, 108.56, 107.41, 103.43, 66.74, 60.75, 56.12, 51.83, 47.48, 17.54, 12.37, 11.53.

*4.1.10.6. N-{5-[3-(dimethylamino)propoxy]-2-methylphenyl}-N′-{3′-hydroxy-4′-[(1E)-N-hydroxyethanimidoyl]-5,6-dimethoxybiphenyl-3-yl}urea (**12g**).* mp.: 181–182 °C. EI-MS (*m/z*): 536.3 (M^+). ^{1}H NMR (400 MHz, $(CD_3)_2SO$) δ 9.61 (s, 1H), 8.20 (s, 1H), 7.56 (s, 1H), 7.52 (d, *J* = 4 Hz, 1H), 7.25 (s, 1H), 7.04 (s, 1H), 7.02 (s, 1H), 6.99 (s, 1H), 6.97 (s, 1H), 6.50 (m, *J* = 6 Hz, 1H), 3.92 (t, *J* = 6 Hz, 2H), 3.83 (s, 3H), 3.50 (s, 3H), 2.34 (t, *J* = 8 Hz, 2H), 2.18 (s, 3H), 2.13 (s, 6H), 1.81 (m, *J* = 12 Hz, 2H).

*4.1.10.7. N-{3′-hydroxy-4′-[(1E)-N-hydroxyethanimidoyl]-5,6-dimethoxybiphenyl-3-yl}-N′-[2-methyl-5-(2-piperidin-1-ylethoxy) phenyl]urea (**12h**).* mp.: 162–164 °C. EI-MS (*m*/*z*): 564.1 (M^+). ^{1}H NMR (400 MHz, $(CD_3)_2SO$) δ 11.65 (s, 1H), 11.62 (s, 1H), 9.19 (s, 1H), 7.89 (s, 1H), 7.59 (s, 1H), 7.55 (d, *J* = 4 Hz, 1H), 7.21 (s, 1H), 7.03 (s, 1H), 7.01 (s, 1H), 6.99 (s, 1H), 6.51 (m, *J* = 6 Hz, 1H), 3.99 (t, *J* = 6 Hz, 2H), 3.84 (s, 3H), 3.50 (s, 3H), 2.63 (t, *J* = 6 Hz, 2H), 2.42 (s, 4H), 2.30 (s, 3H), 2.17 (s, 3H), 1.49 (s, 4H), 1.37 (d, *J* = 4 Hz, 2H). ^{13}C NMR (101 MHz, $(CD_3)_2SO$) δ 157.68, 157.42, 157.21, 153.31, 153.06, 141.20, 140.32, 138.70, 136.52, 134.54, 131.01, 128.15, 120.09, 119.05, 118.74, 117.25, 111.36, 108.48, 107.43, 103.43, 65.97, 60.75, 57.88, 56.12, 54.90, 26.04, 24.39, 17.53, 11.53.

*4.1.10.8. N-{3′-hydroxy-4′-[(1E)-N-hydroxyethanimidoyl]-5,6-dimethoxybiphenyl-3-yl}-N′-[2-methyl-5-(2-pyrrolidin-1-ylethoxy) phenyl]urea (**12i**).* mp.: 144–146 °C. EI-MS (*m*/*z*): 548.3 (M^+). ^{1}H NMR (400 MHz, $(CD_3)_2SO$) δ 11.63 (d, *J* = 6 Hz, 1H), 9.17 (s, 1H), 7.89 (d, *J* = 4 Hz, 1H), 7.61 (d, *J* = 4 Hz, 1H), 7.47 (d, *J* = 4 Hz, 1H), 7.43 (d, *J* = 4 Hz, 1H), 7.25 (s, 1H), 7.06 (d, *J* = 2 Hz, 1H), 6.99 (d, *J* = 2 Hz, 1H), 6.52 (d, *J* = 4 Hz, 1H), 5.20 (s, 1H), 4.00 (t, *J* = 6 Hz, 2H), 3.84 (s, 3H), 3.50 (d, *J* = 6 Hz, 3H), 2.78 (d, *J* = 2 Hz, 2H), 2.51 (s, 4H), 2.17 (s, 3H), 2.10 (d, *J* = 6 Hz, 3H), 1.67 (d, *J* = 2 Hz, 4H).

*4.1.10.9. N-{3′-hydroxy-4′-[(1E)-N-hydroxyethanimidoyl]-5,6-dimethoxybiphenyl-3-yl}-N′-[2-methyl-5-(3-morpholin-4-ylpropoxy) phenyl]urea (**12j**).* mp.: 202–203 °C. EI-MS (*m*/*z*): 578.4 (M^+). ^{1}H NMR (400 MHz, $(CD_3)_2SO$) δ 11.63 (d, *J* = 6 Hz, 1H), 11.07 (s, 1H), 9.14 (s, 1H), 7.87 (d, *J* = 4 Hz, 1H), 7.59 (d, *J* = 4 Hz, 1H), 7.46 (d, *J* = 4 Hz, 1H), 7.42 (d, *J* = 4 Hz, 1H), 7.24 (d, *J* = 2 Hz, 1H), 7.04 (d, *J* = 4 Hz, 1H), 6.98 (s, 1H), 6.50 (d, *J* = 4 Hz, 1H), 5.19 (s, 1H), 3.93 (t, *J* = 6 Hz, 2H), 3.86 (s, 3H), 3.57 (s, 4H), 3.49 (d, *J* = 6 Hz, 3H), 2.40 (t, *J* = 6 Hz, 2H), 2.30 (s, 4H), 2.16 (s, 3H), 2.08 (s,3H), 1.83 (m, *J* = 14 Hz, 2H).

*4.1.10.10. N-{4-[2-(diethylamino)ethoxy]-2-fluorophenyl}-N′-{3′-hydroxy-4′-[(1E)-N-hydroxyethanimidoyl]-5,6-dimethoxybiphenyl-3-yl}urea (**12k**).* mp.: 163–165 °C. EI-MS (*m*/*z*): 554.2 (M^+). ^{1}H NMR (400 MHz, $(CD_3)_2SO$) δ 11.64 (s, 2H), 8.90 (s, 2H), 7.54 (d, *J* = 4 Hz, 1H),7.47 (d, *J* = 6 Hz, 1H), 7.27 (s, 1H), 7.08 (d, *J* = 4 Hz, 2H), 7.01 (d, *J* = 4 Hz, 1H), 6.98 (s, 1H), 6.97 (s, 1H), 4.03 (t, *J* = 6 Hz, 2H), 3.83 (s, 3H), 3.50 (s, 3H), 2.76 (t, *J* = 6 Hz, 2H), 2.54 (m, *J* = 12 Hz, 4H), 2.30 (s, 3H), 0.97 (t, *J* = 8 Hz,6H).

*4.1.10.11. N-{4-[3-(dimethylamino)propoxy]-2-fluorophenyl}-N′-{3′-hydroxy-4′-[(1E)-N-hydroxyethanimidoyl]-5,6-dimethoxybiphenyl-3-yl}urea (**12l**).* mp.: 204–205 °C. EI-MS (*m*/*z*): 550.1 (M^+). ^{1}H NMR (400 MHz, $(CD_3)_2SO$) δ 11.70 (s, 2H), 8.91 (s, 2H), 7.53 (d, *J* = 4 Hz, 1H),7.47 (d, *J* = 6 Hz, 1H), 7.27 (s, 1H), 7.07 (s, 1H), 7.06 (s, 1H), 7.00 (d, *J* = 4 Hz, 1H), 6.97 (s, 1H), 6.95 (s, 1H), 4.01 (t, *J* = 6 Hz, 2H), 3.82 (s, 3H), 3.50 (s, 3H), 2.34 (t, *J* = 8 Hz, 2H), 2.29 (s, 3H), 2.13 (s, 6H), 1.83 (t, *J* = 12 Hz, 2H). ^{13}C NMR (101 MHz, $(CD_3)_2SO$) δ 157.60, 157.25, 153.21, 141.63, 141.52, 141.17, 140.28, 136.51, 134.48, 134.11, 128.12, 120.05, 118.78, 117.25, 116.24, 114.59, 111.57, 107.47, 107.24, 103.66, 67.98, 60.74, 56.11, 56.01, 45.66, 27.43, 11.54.

*4.1.10.12. N-[2-fluoro-4-(2-piperidin-1-ylethoxy)phenyl]-N′-{3′-hydroxy-4′-[(1E)-N-hydroxyethanimidoyl]-5,6-dimethoxybiphenyl-3-yl}urea (**12m**).* mp.: 120–122 °C. EI-MS (*m*/*z*): 566.1 (M^+). ^{1}H NMR (400 MHz, $(CD_3)_2SO$) δ 11.64 (s, 2H), 8.94 (s, 2H), 7.54 (d, *J* = 4 Hz, 1H),7.47 (d, *J* = 6 Hz, 1H), 7.27 (s, 1H), 7.11 (d, *J* = 4 Hz, 2H), 7.08 (s, 1H),7.01 (d, *J* = 4 Hz, 1H), 6.98 (s, 1H), 6.97 (s, 1H), 4.08 (t, *J* = 6 Hz, 2H), 3.83 (s, 3H), 3.50 (s, 3H), 2.64 (t, *J* = 6 Hz, 2H), 2.42 (s, 4H), 2.30 (s, 3H), 1.49 (m, *J* = 12 Hz,4H), 1.37 (d, *J* = 2 Hz, 2H).

*4.1.10.13. N-[2-fluoro-4-(2-pyrrolidin-1-ylethoxy)phenyl]-N′-{3′-hydroxy-4′-[(1E)-N-hydroxyethanimidoyl]-5,6-dimethoxybiphenyl-3-yl}urea (**12n**).* mp.: 174–176 °C. EI-MS (*m*/*z*): 552.2 (M^+). ^{1}H NMR (400 MHz, $(CD_3)_2SO$) δ 11.80 (s, 1H), 10.48 (s, 1H), 7.53 (t, *J* = 8 Hz, 2H),7.41 (s, 1H), 7.11 (d, *J* = 4 Hz, 1H), 7.07 (d, *J* = 4 Hz, 1H), 6.99 (d, *J* = 4 Hz, 1H), 6.96 (d, *J* = 4 Hz, 2H), 4.07 (t, *J* = 6 Hz, 2H), 3.81 (s, 3H), 3.49 (s, 3H), 2.77 (t, *J* = 6 Hz, 2H), 2.51 (s, 4H), 2.28 (s, 3H), 1.68 (s, 4H).

*4.1.10.14. N-[2-fluoro-4-(2-morpholin-4-ylethoxy)phenyl]-N′-{3′-hydroxy-4′-[(1E)-N-hydroxyethanimidoyl]-5,6-dimethoxybiphenyl-3-yl}urea (**12o**).* mp.: 195–197 °C. EI-MS (*m*/*z*): 568.4 (M^+). ^{1}H NMR (400 MHz, $(CD_3)_2SO$) δ 9.24 (s, 2H), 7.50 (d, *J* = 2 Hz, 1H), 7.48 (s, 1H), 7.28 (d, *J* = 2 Hz, 1H), 7.07 (t, *J* = 10 Hz, 2H), 6.95 (d, *J* = 4 Hz, 3H), 4.10 (t, *J* = 6 Hz, 2H), 3.82 (s, 3H), 3.58 (t, *J* = 6 Hz, 2H), 3.49 (s, 3H), 2.68 (t, *J* = 4 Hz, 2H), 2.47 (t, *J* = 4 Hz, 2H), 2.29 (s, 3H), 2.30 (s, 3H). ^{13}C NMR (101 MHz, $(CD_3)_2SO$) δ 157.58, 157.29, 153.26; 153.21, 141.39, 141.28, 141.12, 140.28, 136.58, 134.49, 128.11, 120.02, 118.80, 117.25, 116.35, 114.46, 111.49, 107.33, 107.11, 103.57, 67.60, 66.65, 60.74, 57.48, 56.11, 54.08, 11.55.

*4.1.10.15. N-[2-fluoro-4-(3-morpholin-4-ylpropoxy)phenyl]-N′-{3′-hydroxy-4′-[(1E)-N-hydroxyethanimidoyl]-5,6-dimethoxybiphenyl-3-yl}urea (**12p**).* mp.: 207–208 °C. EI-MS (*m*/*z*): 582.3 (M^+). ^{1}H NMR (400 MHz, $(CD_3)_2SO$) δ 11.52 (s, 2H), 9.41 (s, 2H), 7.54 (d, *J* = 2 Hz, 1H), 7.49 (d, *J* = 8 Hz, 1H), 7.31 (s, 1H), 7.07 (s, 1H), 7.06 (s, 1H), 7.01 (m, *J* = 6 Hz, 1H), 6.97 (s, 1H), 6.95 (s, 1H), 4.02 (t, *J* = 6 Hz, 2H), 3.82 (s, 3H), 3.57 (t, *J* = 4 Hz, 2H), 3.50 (s, 3H), 2.41 (t, *J* = 6 Hz, 2H), 2.36 (s, 4H), 2.29 (s, 3H), 1.86 (m, *J* = 12 Hz,2H). ^{13}C NMR (101 MHz, $(CD_3)_2SO$) δ 157.57, 157.31, 153.31, 153.19, 141.48, 141.37, 141.09, 140.29, 136.67, 134.47, 128.09, 120.00, 118.79, 117.26, 116.25, 114.52, 111.52, 107.37, 107.14, 103.58, 67.98, 66.67, 60.73, 56.09, 55.21, 53.83, 26.41, 11.54.

*4.1.10.16. N-{2-chloro-4-[2-(diethylamino)ethoxy]phenyl}-N′-{3′-hydroxy-4′-[(1E)-N-hydroxyethanimidoyl]-5,6-dimethoxybiphenyl-3-yl}urea (**12q**).* mp.: 136–138 °C. EI-MS (*m*/*z*): 570.2 (M^+). ^{1}H NMR (400 MHz, $(CD_3)_2SO$) δ 11.64 (s, 1H), 11.61 (s, 1H), 7.54 (d, *J* = 4 Hz, 1H), 7.35 (d, *J* = 4 Hz, 1H), 7.26 (s, 1H), 7.09 (d, *J* = 4 Hz, 1H), 7.01 (d, *J* = 4 Hz, 1H), 6.98 (s, 1H), 6.95 (s, 1H), 6.87 (d, *J* = 4 Hz, 1H), 4.03 (d, *J* = 12 Hz, 2H), 3.83 (s, 3H), 3.50 (s, 3H), 2.61 (s, 2H), 2.51 (s, 4H), 2.29 (s, 3H), 1.00 (t, *J* = 6 Hz,2H).

*4.1.10.17. N-{2-chloro-4-[3-(dimethylamino)propoxy]phenyl}-N′-{3′-hydroxy-4′-[(1E)-N-hydroxyethanimidoyl]-5,6-dimethoxybiphenyl-3-yl}urea (**12r**).* mp.: 176–178 °C. EI-MS (*m*/*z*): 556.2 (M^+). ^{1}H NMR (400 MHz, $(CD_3)_2SO$) δ 11.66 (s, 2H), 8.73 (s, 1H), 8.59 (s, 1H), 7.54 (d, *J* = 4 Hz, 1H), 7.35 (d, *J* = 6 Hz, 1H), 7.27 (s, 1H), 7.01 (d, *J* = 4 Hz, 1H), 6.98 (s, 1H), 6.96 (s, 1H), 6.86 (s, 1H), 6.83 (s, 1H), 3.94 (d, *J* = 6 Hz, 2H), 3.82 (s, 3H), 3.49 (s, 3H), 2.34 (d, *J* = 8 Hz, 2H), 2.29 (s, 3H), 2.14 (s, 6H), 1.83 (t, *J* = 10 Hz,2H).

*4.1.10.18. N-[2-chloro-4-(2-piperidin-1-ylethoxy)phenyl]-N′-{3′-hydroxy-4′-[(1E)-N-hydroxyethanimidoyl]-5,6-dimethoxybiphenyl-3-yl}urea (**12s**).* mp.: 147–149 °C. EI-MS (*m*/*z*): 582.2 (M^+). ^{1}H NMR (400 MHz, $(CD_3)_2SO$) δ 11.66 (s, 1H), 11.65s, 1H), 9.53 (s, 1H), 9.36 (s, 1H), 7.54 (d, *J* = 4 Hz, 1H), 7.37 (d, *J* = 4 Hz, 1H), 7.32 (s, 1H), 7.00 (d, *J* = 4 Hz, 1H), 6.96 (s, 1H), 6.90 (s, 2H), 6.87 (s, 1H), 4.17 (s, 2H), 3.82 (s, 3H), 3.49 (s, 3H), 3.38 (s, 2H), 2.51 (s, 4H), 2.29 (s, 3H), 1.62 (s, 4H), 1.43 (s, 2H).

*4.1.10.19. N-[2-chloro-4-(2-pyrrolidin-1-ylethoxy)phenyl]-N′-{3′-hydroxy-4′-[(1E)-N-hydroxyethanimidoyl]-5,6-dimethoxybiphenyl-3-yl}urea (**12t**).* mp.: 108–110 °C. EI-MS (*m*/*z*): 568.2 (M^+). ^{1}H NMR (400 MHz, $(CD_3)_2SO$) δ 11.64 (d, *J* = 4 Hz, 1H), 8.85s, 2H), 7.46 (s, 1H), 7.42 (d, *J* = 4 Hz, 1H), 7.35 (d, *J* = 4 Hz, 1H), 7.30 (s, 1H), 7.23 (s, 1H), 7.09 (d, *J* = 4 Hz, 1H), 7.03 (d, *J* = 6 Hz, 1H), 6.94 (s, 1H), 5.20 (s, 1H),

4.09 (t, J = 6 Hz, 2H), 3.83 (s, 3H), 3.49 (d, J = 6 Hz, 3H), 2.80 (t, J = 4 Hz, 2H), 2.55 (s, 4H), 2.10 (d, J = 4 Hz, 3H), 1.68 (s, 4H).

*4.1.10.20. N-[2-chloro-4-(2-morpholin-4-ylethoxy)phenyl]-N′-{3′-hydroxy-4′-[(1E)-N-hydroxyethanimidoyl]-5,6-dimethoxybiphenyl-3-yl}urea (**12u**).* mp.: 122–124 °C. EI-MS (m/z): 584.1 (M^+). ^{1}H NMR (400 MHz, $(CD_3)_2SO$) δ 11.65 (s, 1H), 11.61 (s, 1H), 7.54 (d, J = 4 Hz, 1H), 7.34 (d, J = 6 Hz, 1H), 7.26 (s, 1H), 7.10 (d, J = 4 Hz, 1H), 7.01 (d, J = 6 Hz, 1H), 6.98 (s, 1H), 6.96 (d, J = 2 Hz, 1H), 6.87 (d, J = 4 Hz, 1H), 4.12 (t, J = 4 Hz, 1H), 4.03 (t, J = 6 Hz, 1H), 3.83 (s, 3H), 3.58 (d, J = 2 Hz, 4H), 3.50 (s, 3H), 2.69 (m, J = 14 Hz, 2H), 2.51 (s, 4H), 2.30 (s, 3H). ^{13}C NMR (101 MHz, $(CD_3)_2SO$) δ 157.69, 157.19, 153.24, 153.14, 149.37, 141.27, 141.10, 140.29, 136.36, 134.46, 134.09, 128.16, 121.75, 120.57, 120.11, 118.75, 117.24, 115.11, 111.68, 103.81, 67.72, 66.67, 60.75, 57.33, 56.14, 54.17, 11.55.

*4.1.10.21. N-[2-chloro-4-(3-morpholin-4-ylpropoxy)phenyl]-N′-{3′-hydroxy-4′-[(1E)-N-hydroxyethanimidoyl]-5,6-dimethoxybiphenyl-3-yl}urea (**12v**).* mp.: 211–213 °C. EI-MS (m/z): 598.2 (M^+). ^{1}H NMR (400 MHz, $(CD_3)_2SO$) δ 11.65 (s, 1H), 11.63 (s, 1H), 9.29 (s, 1H), 9.14 (s, 1H), 7.54 (d, J = 4 Hz, 1H), 7.38 (d, J = 6 Hz, 1H), 7.30 (d, J = 2 Hz, 1H), 7.00 (d, J = 4 Hz, 1H), 6.97 (s, 1H), 6.93 (d, J = 2 Hz, 1H), 6.89 (s, 1H), 6.87 (s, 1H), 4.01 (t, J = 6 Hz, 2H), 3.95 (d, J = 6 Hz, 4H), 3.82 (s, 3H), 3.49 (s, 3H), 3.45 (d, J = 6 Hz, 2H), 3.24 (s, 2H), 3.07 (s, 2H), 2.29 (s, 3H), 2.18 (m, J = 8 Hz, 2H).

*4.1.10.22. N-{3′-hydroxy-4′-[(1E)-N-hydroxyethanimidoyl]-5,6-dimethoxybiphenyl-3-yl}-N′-[4-(piperidin-1-ylmethyl)phenyl]urea (**12w**).* mp.: 153–155 °C. EI-MS (m/z): 518.3 (M^+). ^{1}H NMR (400 MHz, $(CD_3)_2SO$) δ 11.67 (s, 2H), 9.10 (s, 1H), 9.03 (s, 1H), 7.54 (d, J = 4 Hz, 1H), 7.41 (s, 1H), 7.38 (s, 1H), 7.30 (s, 1H), 7.17 (s, 1H), 7.15 (s, 1H), 7.00 (d, J = 4 Hz, 1H), 6.97 (s, 1H), 6.95 (s, 2H), 3.82 (s, 3H), 3.50 (s, 3H), 3.33 (s, 2H), 2.29 (s, 7H), 1.46 (d, J = 2 Hz, 4H), 1.38 (s, 2H). ^{13}C NMR (101 MHz, $(CD_3)_2SO$) δ 157.62, 157.22, 153.28, 153.23, 141.04, 140.33, 138.99, 136.74, 134.48, 132.20, 129.68, 128.13, 120.08, 118.76, 118.33, 117.24, 111.31, 103.39, 62.97, 60.75, 56.10, 54.27, 26.03, 24.55, 11.55.

*4.1.10.23. N-{3′-hydroxy-4′-[(1E)-N-hydroxyethanimidoyl]-5,6-dimethoxybiphenyl-3-yl}-N′-[4-(morpholin-4-ylmethyl)phenyl]urea (**12x**).* mp.: 153–155 °C. EI-MS (m/z): 520.1 (M^+). ^{1}H NMR (400 MHz, $(CD_3)_2SO$) δ 11.65 (s, 1H), 11.61 (s, 1H), 8.68 (s, 1H), 8.66 (s, 1H), 7.55 (d, J = 4 Hz, 1H), 7.42 (s, 1H), 7.40 (s, 1H), 7.26 (s, 1H), 7.21 (s, 1H), 7.19 (s, 1H), 7.02 (d, J = 4 Hz, 1H), 6.98 (s, 1H), 6.97 (d, J = 2 Hz, 2H), 3.83 (s, 3H), 3.56 (s, 4H), 3.50 (s, 3H), 3.38 (s, 2H), 2.33 (s, 4H), 2.30 (s, 3H).

*4.1.10.24. N-{3′-hydroxy-4′-[(1E)-N-hydroxyethanimidoyl]-5,6-dimethoxybiphenyl-3-yl}-N′-{4-[(4-methylpiperazin-1-yl)methyl]phenyl}urea (**12y**).* mp.: 189–190 °C. EI-MS (m/z): 533.2 (M^+). ^{1}H NMR (400 MHz, $(CD_3)_2SO$) δ 11.69 (s, 2H), 10.00 (s, 1H), 9.93 (s, 1H), 7.54 (d, J = 4 Hz, 1H), 7.44 (s, 1H), 7.42 (s, 1H), 7.38 (s, 1H), 7.16 (s, 1H), 7.14 (s, 1H), 7.00 (d, J = 4 Hz, 1H), 6.96 (s, 2H), 3.82 (s, 3H), 3.49 (s, 3H), 3.36 (s, 2H), 2.51 (s, 4H), 2.29 (s, 7H), 2.14 (s, 3H). ^{13}C NMR (101 MHz, $(CD_3)_2SO$) δ 157.52, 157.18, 153.60, 153.14, 140.78, 140.40, 139.57, 137.21, 134.43, 131.44, 129.67, 128.10, 120.09, 118.75, 118.20, 117.22, 111.18, 103.25, 62.24, 60.75, 56.09, 55.19, 52.95, 46.22, 11.56.

*4.1.10.25. N-{4′-[(1E)-N-hydroxyethanimidoyl]-3′,5,6-trimethoxybiphenyl-3-yl}-N′-[4-(piperidin-1-ylmethyl)phenyl]urea (**12w′**).* mp.: 118–120 °C. EI-MS (m/z): 532.3 (M^+). ^{1}H NMR (400 MHz, $(CD_3)_2SO$) δ 11.07 (s, 1H), 8.73 (s, 1H), 8.69 (s, 1H), 7.40 (s, 1H), 7.38 (s, 1H), 7.33 (d, J = 2 Hz, 1H), 7.27 (d, J = 4 Hz, 1H), 7.18 (s, 1H), 7.16 (s, 1H), 7.13 (s, 1H), 7.03 (d, J = 4 Hz, 1H), 6.93 (s, 1H), 3.84 (s, 6H), 3.55 (s, 3H), 3.34 (s, 2H), 2.29 (s, 4H), 2.10 (s, 3H), 1.47 (d, J = 4 Hz,4H), 1.37 (s, 2H).

*4.1.10.26. N-{4′-[(1E)-N-hydroxyethanimidoyl]-3′,5,6-trimethoxybiphenyl-3-yl}-N′-[4-(morpholin-4-ylmethyl)phenyl]urea (**12x′**).* mp.: 169–171 °C. EI-MS (m/z): 534.3 (M^+). ^{1}H NMR (400 MHz, $(CD_3)_2SO$) δ 11.07 (s, 1H), 8.68 (s, 2H), 7.41 (s, 1H), 7.39 (s, 1H), 7.33 (s, 1H), 7.27 (d, J = 2 Hz, 1H), 7.21 (s, 1H), 7.19 (s, 1H), 7.13 (s, 1H), 7.03 (d, J = 4 Hz, 1H), 6.93 (s, 1H), 3.84 (s, 6H), 3.55 (s, 7H), 3.38 (s, 2H), 2.33 (s, 4H), 2.09 (s, 3H).

*4.1.10.27. N-{4′-[(1E)-N-hydroxyethanimidoyl]-3′,5,6-trimethoxybiphenyl-3-yl}-N′-{4-[(4-methylpiperazin-1-yl)methyl]phenyl}urea (**12y′**).* mp.: 109–111 °C. EI-MS (m/z): 547.3 (M^+). ^{1}H NMR (400 MHz, $(CD_3)_2SO$) δ 11.08 (s, 1H), 8.74 (s, 1H), 8.72 (s, 1H), 7.41 (s, 1H), 7.39 (s, 1H), 7.33 (s, 1H), 7.27 (d, J = 4 Hz, 1H), 7.19 (s, 1H), 7.17 (s, 1H), 7.13 (s, 1H), 7.04 (d, J = 4 Hz, 1H), 6.93 (s, 1H), 3.84 (s, 6H), 3.55 (s, 3H), 3.37 (s, 2H), 2.31 (s, 8H), 2.14 (s, 3H), 2.10 (s, 3H).

4.2. Kinase assay [20]

The ability of compounds to inhibit the phosphorylation of a peptide substrate by VEGFR-2 was evaluated in a microtiter plate format using homogenous time-resolved fluorescence (HTRF). Firstly, 2 μL kinase (Km = 0.003767 ng/μL) and 2 μL substrate (Km = 121.4 nM) were separately added to a 384-well plate, and variable concentrations of compounds (diluted in buffer) were then added to the assay plate. ATP (2 μL, Km = 1.332 μM) was added and the reaction was allowed to proceed at 37 °C for 30 min. The TK-Antibody labeled with Eu^{3+}-cryptate and streptavidin- XL665 were then added with EDTA to detect the phosphorylated product at room temperature for 1 h. Then the fluorescence was measured at 615 nm (cryptate) and 665 nm (XL665) using the Perkin–Elmer victor 2030 multilabel plate reader. Finally, the results were calculated as follows: ratio = (OD665 nm/OD615 nm) × 10^4.

4.3. Cell growth inhibitory activity in cancer cell lines [21]

Growth inhibitory activities were evaluated on the following cell lines: A549, MCF-7, ECV304, MDA-MB-435S, H1299, MDA-MB-231, A375, HT29, and SMMC-7721. Eight potent VEGFR-2 inhibitors were evaluated using MTT assay to assess cell proliferation. Exponentially growing cells were harvested and plated in 96-well plates at a concentration of 1 × 10^4 cells/well, and then incubated for 24 h at 37 °C. The cells in wells were treated with title compounds respectively at various concentrations for 48 h. Then, 20 mL MTT (5 mg/mL) was added to each well and incubated for 4 h at 37 °C. Supernatant was discarded, and 150 mL DMSO was added to each well. Absorbance values were determined by a microplate reader (Bio-Rad Instruments) at 490 nm. The IC_{50} values were calculated according to inhibition ratios.

4.4. Molecular docking modeling [22]

In order to understand the binding mode of inhibitors with VEGFR-2, molecule docking was performed using Sybyl/Surflex-dock based on the crystal structures of VEGFR-2 (PDB ID: 3C7Q). Hydrogen was added and minimized using the Tripos force field and Pullman charges. Compound (**12p**) was depicted with the Sybyl/Sketch module (Tripos Inc.) and optimized applying Powell's method with the Tripos force field with convergence criterion set at 0.05 kcal/(Åmol), and assigned with the Gasteiger–Hückel method. The residues in a radius 5.0 Å around BIBF1120 (the ligand of VEGFR-2 in the crystal complex) were selected as the active site. Other docking parameters were kept at default.

Acknowledgment

This work was supported by the National Natural Science Foundation of China (Grant no. 81302641 and 81302737) and the Fundamental Research Funds for the Central Universities (xjj2014140).

Appendix A. Supplementary data

Supplementary data related to this article can be found at http://dx.doi.org/10.1016/j.ejmech.2014.11.032.

References

[1] F. Ciardiello, R. Caputo, R. Bianco, V. Damiano, G. Fontanini, S. Cuccato, S. De Placido, A.R. Bianco, G. Tortora, Inhibition of growth factor production and angiogenesis in human cancer cells by ZD1839 (Iressa), a selective epidermal growth factor receptor tyrosine kinase inhibitor, Clin. Cancer Res. 7 (2001) 1459–1465.
[2] N. Ferrara, H.P. Gerber, J. LeCouter, The biology of VEGF and its receptors, Nat. Med. 9 (2003) 669–676.
[3] L. Shi, T.T. Wu, Z. Wang, J.Y. Xue, Y.G. Xu, Discovery of N-(2-phenyl-1H-benzo [d] imidazol-5-yl)quinolin-4-amine derivatives as novel VEGFR-2 kinase inhibitors, Eur. J. Med. Chem. 84 (2014) 698–707.
[4] J. Zhang, Y. Shan, X. Pan, L. He, Recent advances in antiangiogenic agents with VEGFR as target, Mini Rev. Med. Chem. 11 (2011) 920–946.
[5] M.L. Barbosa, L.M. Lima, R. Tesch, C.M. Sant'Anna, F. Totzke, M.H. Kubbutat, C. Schächtele, S.A. Laufer, E.J. Barreiro, Novel 2-chloro-4-anilino-quinazoline derivatives as EGFR and VEGFR-2 dual inhibitors, Eur. J. Med. Chem. 71 (2014) 1–14.
[6] S. Wilhelm, C. Carter, M. Lynch, Discovery and development of sorafenib: a multikinase inhibitor for treating cancer, Nat. Rev. Drug Discov. 5 (2006) 835–845.
[7] D.H. Albert, P. Tapang, T.J. Magoc, Preclinical activity of ABT-869, a multitargeted receptor tyrosine kinase inhibitor, Mol. Cancer. Ther. 5 (2006) 995–1006.
[8] T.A. Fong, L.K. Shawver, L. Sun, C. Tang, H. App, T.J. Powell, Y.H. Kim, R. Schreck, X. Wang, W. Risau, A. Ullrich, K.P. Hirth, G. McMahon, SU5416 is a potent and selective inhibitor of the vascular endothelial growth factor receptor (Flk-1/KDR) that inhibits tyrosine kinase catalysis, tumor vascularization, and growth of multiple tumor types, Cancer Res. 59 (1999) 99–106.
[9] Q.D. Nguyen, S. Rodrigues, C.M. Rodrigue, C. Rivat, C. Grijelmo, E. Bruyneel, S. Emami, S. Attoub, C. Gespach, Inhibition of vascular endothelial growth factor (VEGF)-165 and semaphorin 3A-mediated cellular invasion and tumor growth by the VEGF signaling inhibitor ZD4190 in human colon cancer cells and xenografts, Mol. Cancer Ther. 5 (2006) 2070–2077.
[10] C. Wang, H. Gao, J. Dong, F. Wang, P. Li, J. Zhang, Insight into the medicinal chemistry of EGFR and HER-2 inhibitors, Curr. Med. Chem. 21 (2014) 1336–1350.
[11] C. Wang, J. Dong, Y. Zhang, F. Wang, H. Gao, P. Li, S. Wang, J. Zhang, Design, synthesis and biological evaluation of biphenyl urea derivatives as novel VEGFR-2 inhibitors, MedChemComm 4 (2013) 1434–1438.
[12] W. Deng, Z. Guo, Y. Guo, Z. Feng, Y. Jiang, F. Chu, Acryloylamino-salicylanilides as EGFR PTK inhibitors, Bioorg. Med. Chem. Lett. 16 (2006) 469–472.
[13] C. Wang, H. Gao, J. Dong, Y. Zhang, P. Su, Y. Shi, J. Zhang, Biphenyl derivatives incorporating urea unit as novel VEGFR-2 inhibitors: design, synthesis and biological evaluation, Bioorg. Med. Chem. 22 (2014) 277–284.
[14] J. Zhang, Y.M. Zhang, Y. Shan, N. Li, W. Ma, L. He, Synthesis and preliminary biological evaluation of novel taspine derivatives as anticancer agents, Eur. J. Med. Chem. 45 (2010) 2798–2805.
[15] J.Q. Wang, M.Z. Gao, K.D. Miller, G.W. Sledge, Q.H. Zheng, Synthesis of [11C] Iressa as a new potential PET cancer imaging agent for epidermal growth factor receptor tyrosine kinase, Bioorg. Med. Chem. Lett. 16 (2006) 4102–4106.
[16] J.K. Lynch, J.C. Freeman, A.S. Judd, R. Iyengar, M. Mulhern, G. Zhao, J.J. Napier, D. Wodka, S. Brodjian, B.D. Dayton, D. Falls, C. Ogiela, R.M. Reilly, T.J. Campbell, J.S. Polakowski, L. Hernandez, K.C. Marsh, R. Shapiro, V. Knourek-Segel, B. Droz, E. Bush, M. Brune, L.C. Preusser, R.M. Fryer, G.A. Reinhart, K. Houseman, G. Diaz, A. Mikhail, J.T. Limberis, H.L. Sham, C.A. Collins, P.R. Kym, Optimization of chromone-2-carboxamide melanin concentrating hormone receptor 1 antagonists: assessment of potency, efficacy, and cardiovascular safety, J. Med. Chem. 49 (2006) 6569–6584.
[17] T. Ishiyama, M. Murata, N. Miyaura, Palladium(0)-catalyzed cross-coupling reaction of alkoxydiboron with haloarenes: a direct procedure for arylboronic esters, J. Org. Chem. 60 (1995) 7508–7510.
[18] B.I. Alo, A. Kandil, P.A. Patil, M.J. Sharp, M.A. Siddiqui, V. Snieckus, P.D. Josephy, J. Org. Chem. 56 (1991) 3763–3768.
[19] H. Eckert, J. Auerweck, Solvent-free and safe process for the quantitative production of phosgene from triphosgene by deactivated imino-based catalysts, Org. Process Res. Dev. 14 (2010) 1501–1505.
[20] W. Lu, B.L. Dai, W.N. Ma, Y. Zhang, A novel taspine analog, HMQ1611, inhibits growth of non-small cell lung cancer by inhibiting angiogenesis, Oncol. Lett. 4 (2012) 1109–1113.
[21] F. Wang, W. Lu, T. Zhang, J. Dong, H. Gao, P. Li, S. Wang, J. Zhang, Development of novel ferulic acid derivatives as potent histone deacetylase inhibitors, Bioorg. Med. Chem. 21 (2013) 6973–6980.
[22] J. Zhang, Y. Shan, X. Pan, C. Wang, W. Xu, L. He, Molecular docking, 3D-QSAR studies, and in silico ADME prediction of p-aminosalicylic acid derivatives as neuraminidase inhibitors, Chem. Biol. Drug Des. 78 (2011) 709–717.